Orientational Analysis of Adsorbates in Molecular Sieves by FTIR/ATR Spectroscopy

Mattias Grahn,*,† Antonina Lobanova,† Allan Holmgren,‡ and Jonas Hedlund†

Division of Chemical Technology and Division of Chemistry, Luleå University of Technology, SE-971 87, Luleå, Sweden

Received May 30, 2008. Revised Manuscript Received August 19, 2008

ZnS ATR elements were coated with well-defined *b*-oriented ZSM-5 films by in situ growth. Both adsorption isotherms, as well as molecular orientation of *p*-xylene adsorbed in the films, were measured at 323 and 373 K by FTIR/ATR spectroscopy. The observed isotherms for the *b*-oriented ZSM-5 films in the present work were very similar to previously reported isotherms of supported MFI films, albeit the crystals in the latter films were aluminum free (silicalite-1) and orientated differently relative to the support surface than the crystals in the films studied in the present work. The novel technique facilitated, for the first time, the examination of how the tilt angle varies with loading and temperature. The data obtained in the present work showed that the *p*-xylene molecules were mainly oriented with their long axis parallel to the *b*-direction of the MFI crystals in concert with previously reported results based on FTIR microscopy, Monte Carlo simulations, NMR, and XRD data. At high concentrations, the tilt angle was in good agreement with observations by FTIR microscopy. It was also found that the orientation of the molecules changed with loading, this might be due to different adsorption geometries in the channel intersection as reported previously. The observed tilt angles may also be influenced from competitive adsorption on silanol groups, as was also indicated in the spectra. The results also indicate that the adsorption properties of zeolite films and powders may differ. Hence, adsorption parameters determined for zeolite powders may not necessarily be applicable to films.

Introduction

Zeolites are crystalline aluminosilicates having well-defined pore structure with pore dimensions of similar size as many of the molecules of interest in, for instance, the petrochemical industry. The well-defined pore system of zeolites facilitates their use as molecular sieves for separating molecules based on size or shape of the molecules. In addition, the large surface area of the zeolites together with their adsorption properties enables the separation of different molecules by preferential adsorption.[1−3] Zeolite films have been targeted because of their large potential as selective membranes,[4−10] catalysts,[11−13] components in microelectronic devices,[14] and sensors.[15−20] As a consequence, much effort has been devoted to studying zeolite films in these applications, particularly zeolite membranes for novel separation processes. Despite the large number of publications on zeolite membranes, studies of the adsorption properties of supported zeolite films are scarce, probably because of difficulties in accurately measuring the adsorption in zeolite films with thicknesses typically ranging from 0.5[6,7] to a few micrometers. Consequently, the adsorption parameters determined on zeolite powders have been assumed valid also for supported zeolite films. However, recent XRD studies

* To whom correspondence should be addressed. E-mail: Mattias.Grahn@ltu.se. Fax: 46 920 491 199. Tel: 46 920 491 928.
† Division of Chemical Technology, Luleå University of Technology.
‡ Division of Chemistry, Luleå University of Technology.

(1) Gump, C. J.; Lin, X.; Falconer, J. L.; Noble, R. D. *J. Membr. Sci.* **2000**, *173* (1), 35.
(2) Dong, J.; Lin, Y. S.; Liu, W. *AIChE J.* **2000**, *46* (10), 1957.
(3) Yang, M.; Crittenden, B. D.; Perera, S. P.; Moueddeb, H.; Dalmon, J. A. *J. Membr. Sci.* **1999**, *156* (1), 1.
(4) Bernal, M. P.; Coronas, J.; Menendez, M.; Santamaria, J. *Microporous Mesoporous Mater.* **2003**, *60* (1−3), 99.
(5) Gump, C. J.; Tuan, V. A.; Noble, R. D.; Falconer, J. L. *Ind. Eng. Chem. Res.* **2001**, *40* (2), 565.
(6) Hedlund, J.; Sterte, J.; Anthonis, M.; Bons, A. J.; Carstensen, B.; Corcoran, N.; Cox, D.; Deckman, H.; De Gijnst, W.; de Moor, P. P.; Lai, F.; McHenry, J.; Mortier, W.; Reinoso, J. *Microporous Mesoporous Mater.* **2002**, *52* (3), 179.
(7) Lai, Z.; Bonilla, G.; Diaz, I.; Nery, J. G.; Sujaoti, K.; Amat, M. A.; Kokkoli, E.; Terasaki, O.; Thompson, R. W.; Tsapatsis, M.; Vlachos, D. G. *Science* **2003**, *300*, 456.
(8) Matsufuji, T.; Watanabe, K.; Nishiyama, N.; Egashira, Y.; Matsukata, M.; Ueyama, K. *Ind. Eng. Chem. Res.* **2000**, *39* (7), 2434.
(9) Noack, M.; Mabande, G. T. P.; Caro, J.; Georgi, G.; Schwieger, W.; Kolsch, P.; Avhale, A. *Microporous Mesoporous Mater.* **2005**, *82* (1−2), 147.
(10) Zhu, W.; Hrabanek, P.; Gora, L.; Kapteijn, F.; Moulijn, J. A. *Ind. Eng. Chem. Res.* **2006**, *45* (2), 767.
(11) Hedlund, J.; Ohrman, O.; Msimang, V.; van Steen, E.; Bohringer, W.; Sibya, S.; Moller, K. *Chem. Eng. Sci.* **2004**, *59* (13), 2647.
(12) Li, Y.; Huang, S.; Wu, S.; Yuan, X. *Catal. Lett.* **2003**, *87* (1), 31.
(13) Oudshoorn, O. L.; Janissen, M.; van Kooten, W. E. J.; Jansen, J. C.; van Bekkum, H.; van den Bleek, C. M.; Calis, H. P. A. *Chem. Eng. Sci.* **1999**, *54* (10), 1413.
(14) Li, S. A.; Li, Z. J.; Yan, Y. S. *Adv. Mater.* **2003**, *15* (18), 1528.
(15) Bjorklund, R. B.; Hedlund, J.; Sterte, J.; Arwin, H. *J. Phys. Chem. B* **1998**, *102* (12), 2245.
(16) Grahn, M.; Wang, Z.; Lidstrom-Larsson, M.; Holmgren, A.; Hedlund, J.; Sterte, J. *Microporous Mesoporous Mater.* **2005**, *81* (1−3), 357.
(17) Mintova, S.; Schoeman, B.; Valtchev, V.; Sterte, J.; Mo, S. Y.; Bein, T. *Adv. Mater.* **1997**, *9* (7), 585.
(18) Plog, C.; Maunz, W.; Kurzweil, P.; Obermeier, E.; Scheibe, C. *Sens. Actuators, B* **1995**, *25* (1−3), 403.
(19) Vilaseca, M.; Coronas, J.; Cirera, A.; Cornet, A.; Morante, J. R.; Santamaria, J. *Catal. Today* **2003**, *82* (1−4), 179.
(20) Zhang, J.; Dong, J. H.; Luo, M.; Xiao, H.; Murad, S.; Normann, R. A. *Langmuir* **2005**, *21* (19), 8609.

10.1021/cm801399s CCC: $40.75
Published on Web 09/11/2008

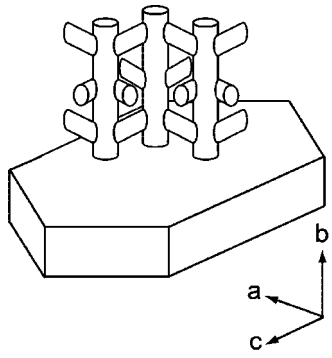

Figure 1. Schematic figure of MFI crystal with channel system and crystallographic axes.

of zeolite membranes[21−23] have shown that the unit-cell parameters differ between zeolite powder and supported films. The observed differences were attributed to strain in the film[23] and it is reasonable to believe that these differences may influence the adsorption properties of the films, at least for molecules with diameters close to the diameter of zeolite channels. One such extensively studied (membranes and adsorption) adsorbate/zeolite system is *p*-xylene/MFI. The kinetic diameter of *p*-xylene[5] is 5.85 Å. MFI crystals have straight channels (5.3×5.6 Å^2) running in the crystallographic *b*-direction that intersect with sinusoidal channels (5.5×5.1 Å^2)[24] running in the crystal *a*-direction, see Figure 1.

Several different techniques have been employed for studying the adsorption of *p*-xylene in MFI crystals, such as gravimetry,[25−27] calorimetry,[28] X-ray powder diffraction,[29−31] solid-state NMR spectroscopy,[32−34] IR spectroscopy,[35] FT-Raman spectroscopy,[36,37] and Monte Carlo simulations.[38−40]

It has been found that *p*-xylene adsorb at two different sites in MFI powder and unsupported films.[29,31,41] At low partial pressures, *p*-xylene adsorbs in the intersections of the two channels with the longest axis of the molecule oriented mainly in the *b*-direction of the crystal At higher partial pressures, the molecules adsorb in the sinusoidal channels, with the longest axis of the molecule oriented in the *a*/*c* plane of the crystal. At temperatures below ca. 353 K, four molecules per unit cell adsorb at the first site in the intersections at low pressure and subsequently, at higher pressures, four molecules adsorb also at the second site in the sinusoidal channels, resulting in a type IV isotherm with a step at half of the saturation loading. At higher temperatures, the molecules adsorb only at the first site, resulting in a type I isotherm. Moreover, it has been shown that the structure of the MFI crystals change during adsorption of aromatic molecules.[30,31] At room temperature, unloaded MFI has monoclinic symmetry. At low loadings (0−2 molecules /unit cell), the framework change gradually to orthorhombic symmetry and in this region the two phases coexists. In the intermediate loading region (2−4 molecules/unit cell), only the orthorhombic phase exists and as the loading is further increased (4−8 molecules/unit cell), the framework changes to a another orthorhombic phase. During this process, the framework is slightly distorted, resulting in more elliptical pores.[31]

The orientation of *p*-xylene inside the pores have been investigated with techniques such as XRD,[31] NMR,[32] and IR microscopy.[35] van Koningsveld et al.[31]reported a tilt angle of 7.5° from the (010) direction for *p*-xylene in the intersections using XRD at room temperature and Fyfe et al.[32] reports a best fitted tilt angle of 0° using NMR. However, these measurements were performed at or below room temperature, and in the case of the NMR measurements, the authors' concluded that completely reliable data could only be obtained at and below 213 K. Moreover, NMR data acquired above room temperature could not be used for structure determinations because of extensive molecular motions. Schüth investigated the orientation of *p*-xylene in large silicalite-1 crystals (380×70 μm^2) at ca. 310 K and reported a tilt angle of 18° from the (010) direction.

FTIR/ATR (Fourier transform infrared/attenuated total reflection) spectroscopy is a technique especially well suited for studying thin films and surfaces.[42−46] We have recently published adsorption data for *p*-xylene and *n*-hexane in MFI films grown from seeds using this technique.[47] It was found that for *n*-hexane the results obtained agreed with findings reported for powder. However, for *p*-xylene, the results differed compared to results reported for powder, in that only

(21) Dong, J.; Lin, Y. S.; Hu, M. Z. C.; Peascoe, R. A.; Payzant, E. A. *Microporous Mesoporous Mater.* **2000**, *34* (3), 241.
(22) Gualtieri, M. L.; Gualtieri, A. F.; Hedlund, J.; Jareman, F.; Sterte, J.; Dapiaggi, M. Accurate Measurement of the Thermal Expansion of MFI Zeolite Membranes by In situ HTXRPD. In Recent Advances. In *The Science And Technology Of Zeolites and Related Materials, Parts A−C*; van Steen, E., Callanan, L., Claeys, M., Eds.; Studies in Surface Science and Catalysis; Elsevier Science, Amsterdam, 2004; Vol. 154, p 703.
(23) Jeong, H. K.; Lai, Z. P.; Tsapatsis, M.; Hanson, J. C. *Microporous Mesoporous Mater.* **2005**, *84* (1−3), 332.
(24) Breck, D. *Zeolite Molecular Sieves*; Krieger Publishing Company: Malabar, India, 1984.
(25) Lee, C. K.; Chiang, A. S. T. *J. Chem. Soc., Faraday Trans.* **1996**, *92*, 3445.
(26) Richards, R. E.; Rees, L. V. C. *Zeolites* **1988**, *8* (1), 35.
(27) Song, L.; Rees, L. V. C. *Microporous Mesoporous Mater.* **2000**, *35−36*, 301.
(28) Thamm, H. *J. Phys. Chem.* **1987**, *91*, 8.
(29) Mentzen, B. F. *Mater. Res. Bull.* **1992**, *27* (8), 953.
(30) Mentzen, B. F.; Gelin, P. *Mater. Res. Bull.* **1995**, *30* (3), 373.
(31) van Koningsveld, H.; Tuinstra, F.; van Bekkum, H.; Jansen, J. C. *Acta Crystallogr., Sect. B* **1989**, *B45*, 423.
(32) Fyfe, C. A.; Diaz, A. C.; Grondey, H.; Lewis, A. R.; Forster, H. *J. Am. Chem. Soc.* **2005**, *127* (20), 7543.
(33) Lefebvre, F.; Mentzen, B. F. *Mater. Res. Bull.* **1994**, *29* (10), 1049.
(34) Reicshman, T. P.; Schmitt, K. D.; Olson, D. H. *J. Phys. Chem.* **1988**, *92*, 5165.
(35) Schüth, F. *J. Phys. Chem.* **1992**, *96*, 7493.
(36) Ashtekar, S.; Hastings, J. J.; Gladden, L. F. *J. Chem. Soc., Faraday Trans.* **1998**, *94* (8), 1157.
(37) Huang, Y. *J. Am. Chem. Soc.* **1996**, *118* (30), 7233.
(38) Li, J.; Talu, O. *J. Chem. Soc., Faraday Trans.* **1993**, *89*, 1683.
(39) Mohanty, S.; Davis, H. T.; McCormick, A. V. *Chem. Eng. Sci.* **2000**, *55* (15), 2779.
(40) Snurr, R. Q.; Bell, A. T.; Theodorou, D. N. *J. Phys. Chem.* **1993**, *97*, 13742.
(41) Xomeritakis, G.; Nair, S.; Tsapatsis, M. *Microporous Mesoporous Mater.* **2000**, *38* (1), 61.
(42) Ding, F. X.; Xie, H.; Arshava, B.; Becker, J. M.; Naider, F. *Biochemistry* **2001**, *40* (30), 8945.
(43) Shin, E.-M.; Koenig, J. L. *Appl. Spectrosc.* **2002**, *56* (10), 1251.
(44) Fredriksson, A.; Larsson, M. L.; Holmgren, A. *J. Colloid Interface Sci.* **2005**, *286* (1), 1.
(45) Keresszegi, C.; Ferri, D.; Mallat, T.; Baiker, A. *J. Phys. Chem. B* **2005**, *109* (2), 958.
(46) Wang, Z.; Grahn, M.; Larsson, M. L.; Holmgren, A.; Sterte, J.; Hedlund, J. *Sens. Actuators, B* **2006**, (115), 685.
(47) Grahn, M.; Holmgren, A.; Hedlund, J. *J. Phys. Chem C* **2008**, *112*, 7717.

about half the saturation loading was reached at temperatures below 353 K, resulting in a type I isotherm. This indicates that the adsorption properties are different for zeolite powders and films for tight-fit molecules such as p-xylene. This phenomenon is further studied in the present work employing the same basic technique, i.e., FTIR/ATR spectroscopy but with two very important differences. In the present work, *b*-oriented films were grown on the ATR waveguides and polarized light was employed. This combination will allow the determination of molecular orientation relative to the zeolite lattice in thin zeolite films for the first time.

Experimental Section

Materials Synthesis. *b*-Oriented ZSM-5 (Si/Al = 37) films were prepared on a trapezoidal ZnS element (50 × 20 × 2 mm^3, 45° cut edges, Spectroscopy Central Ltd., U.K.) using an in situ method; details have been given elsewhere.[48] Prior to synthesis, the elements were cleaned in acetone, ethanol, and distilled water in an ultrasonic bath for 10 min in each solvent. The element was then mounted in a Teflon holder that kept the element vertical during synthesis. The holder and element was subsequently placed in a Teflon-lined stainless steel autoclave and a synthesis solution with a molar composition of 3TPAOH:25SiO_2:1600H_2O:100EtOH:0.25 Al_2O_3:1Na_2O was added. The autoclave was placed in a preheated oven at 150 °C for 5.5 h, after which the autoclave was quenched with water. Thereafter, the sample was rinsed in a 0.1 M ammonia solution overnight. Finally, the films were calcined at 450 °C for 24 h to remove the template molecules.

Characterization. Scanning electron microscopy (SEM) images were recorded of gold coated samples using a Philips XL 30 electron microscope equipped with a LaB_6 electron emission source. X-ray diffraction (XRD) data was recorded using a Siemens D5000 X-ray diffractometer and with a Philips XPERT powder diffractometer. The data was used for phase analysis of the films and for determining the preferential orientation of the crystals in the films. Pole figures were recorded using the latter instrument by scanning φ and Ψ from 0 to 360° and from 0 to 82.5°, respectively. The surface coverage of zeolite crystals on the element was estimated by measuring the krypton adsorption at liquid nitrogen temperature using a Micromeritics ASAP 2010 sorption instrument. The BET surface area and density (450 m^2/g and 1760 kg/m^3) for MFI and the film thickness as determined by SEM was used when estimating the surface coverage.[15] Adsorption data of n-hexane (Sigma 99+%) and p-xylene (Aldrich 99+%) in helium carrier gas (AGA 99.99990%) was recorded by FTIR/ATR spectroscopy using a Bruker IFS 66v/S spectrometer equipped with a liquid nitrogen cooled mercury cadmium telluride (MCT) detector and a gas delivery system and in situ cell as described elsewhere.[16] In the present work, an additional ZnSe wire grid polarizer was used for polarizing the incident IR light. Before each adsorption experiment, the film was activated at 300 °C (heating and cooling rate 1 °C/min) for 4 h under a flow of helium. After drying, the cell was mounted in the spectrometer and background spectra were recorded with and without polarizer by averaging 128 scans. Subsequently, the hydrocarbon was introduced and at equilibrium, spectra were recorded with and without polarizer by averaging 64 scans. Both the concentration and the dichroic ratio for *p*-xylene were determined from the integrated absorbance of the 1518 cm^{-1} band. The concentrations were subsequently determined using a procedure described elsewhere.[47]

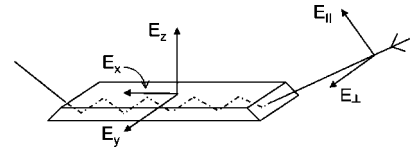

Figure 2. Direction and polarization of the IR beam in the ATR setup.

The Si/Al ratio was determined via ICP-SFMS (inductively coupled plasma−sector field mass spectroscopy) of the ZSM-5 coated ZnS element. The sector field technique is more sensitive than quadrupole instruments and was used since the amount of zeolite was very small compared to the total amount also including the ZnS element. The isotherms for adsorption on silanol groups were determined from the integrated absorbance of the negative band at 3732 cm^{-1}.

Estimation of Molecular Orientation from Spectra. In FTIR/ATR spectroscopy, the IR beam is reflected inside an ATR element, see Figure 2. The electric field of the radiation penetrates a short distance outside the element and interacts with molecules close to the element surface.[49,50]

The intensity of the electric field decreases exponentially with distance (z) from the element surface. The penetration depth, d_p, of the electric field is usually between a couple of hundred nanometers and a few micrometers, making the ATR method especially suited for studying thin films and surfaces and is estimated by

$$d_p = \frac{\lambda/n_1}{2\pi(\sin^2\theta - n_{21}^2)^{1/2}} \quad (1)$$

where λ is the wavelength of the radiation in vacuum and n_1 is the refractive index of the element. Further, the angle of incidence, θ, was 45° during the experiments and $n_{21} = n_2/n_1$ where n_2 is the refractive index of the film. The refractive index of ZnS was taken as 2.25,[51] the refractive index of the gas was set to 1.0.[52] Nair and Tsapatsis reported that the refractive index of a MFI zeolite film changes with loading of an adsorbate.[52] Therefore, a linear model based on their data was set up, where the refractive index increases from 1.22 and 1.32 as the *p*-xylene loading increases in the film.[53] Here it was assumed that the film had a maximum p-xylene loading of 4 molecules per unit cell, as suggested by our previous work.[47] The Lambert−Beer law is not directly applicable in ATR spectroscopy, but a method for estimating the concentration of adsorbed species has been developed.[49,50]

One advantage of the ATR technique is that when combined with polarized radiation it is possible to determine the direction of transition moments of normal vibrations and consequently, to obtain information of the orientation of molecules close to the element. The IR beam is propagating in the $x-z$ plane (plane of incidence), see Figure 2. The surface of the element is in the $x-y$ plane, orthogonal to the plane of incidence. Radiation polarized in the plane of incidence is referred to as parallel- or p-polarized radiation whereas radiation polarized in the plane of the surface is denoted perpendicular- or s-polarized radiation. The ratio of absorbance between s- and p-polarized radiation is denoted the dichroic ratio

(48) Wang, Z.; Hedlund, J.; Zhang, H.; Zou, X. D. *Microporous Mesoporous Mater.* **2006**, *95* (1−3), 86.

(49) Harrick, N. J., *Internal Reflection Spectroscopy*; John Wiley & Sons: New York, 1967.

(50) Mirabella, F. M., Ed. *Internal Reflection Spectroscopy: Theory and Applications.*; Marcel Dekker: New York, 1993.

(51) *Guide for Infrared Spectroscopy*; Bruker Optics: Billerica, MA.

(52) Lide, D., R. Ed. *Handbook of Chemistry and Physics*, 71st ed.; CRC Press; Boca Raton, FL, 1991.

(53) Nair, S.; Tsapatsis, M. *Microporous Mesoporous Mater.* **2003**, *58* (2), 81.

$$D = \frac{A_s}{A_p} \tag{2}$$

and is given by[54]

$$D = \frac{A_s}{A_p} = \frac{E_y^2(\sin^2\gamma(2 - 3\sin^2\Theta) + 2\sin^2\Theta)}{(E_x^2 + E_z^2)2\sin^2\Theta + (2 - 3\sin^2\Theta)(E_x^2\sin^2\gamma + 2E_z^2\cos^2\gamma)} \tag{3}$$

where γ is the angle between the surface-normal and the main axis of the molecule, here defined as the axis going through the CH_3 groups in the *p*-xylene molecule. The angle between the direction of the transition moment and the main axis of the molecule is denoted Θ. For the breathing mode of the aromatic ring at 1518 cm^{-1} the transition moment is in the same direction as the main axis of the molecule,[55] i.e., $\Theta = 0°$, yielding

$$D = \frac{E_y^2\sin^2\gamma}{E_x^2\sin^2\gamma + 2E_z^2\cos^2\gamma} \tag{4}$$

E_x, E_y, and E_z are the electric field components in the *x*-, *y*- and *z*-direction, respectively.

For a three-layer refractive index model (ATR element, film, and gas) the components of the electric field are given by[56]

$$E_x = \frac{2(\cos\theta)(\sin^2\theta - n_{31}^2)^{0.5}}{(1 - n_{31}^2)^{0.5}[(1 + n_{31}^2)\sin^2\theta - n_{31}^2]^{0.5}} \tag{5}$$

$$E_y = \frac{2\cos\theta}{(1 - n_{31}^2)^{0.5}} \tag{6}$$

$$E_z = \frac{2n_{32}^2\sin\theta\cos\theta}{(1 - n_{31}^2)^{0.5}[(1 + n_{31}^2)\sin^2\theta - n_{31}^2]^{0.5}} \tag{7}$$

where n_3 is the refractive index of the gas outside the film and $n_{31} = n_3/n_1$ and $n_{32} = n_3/n_2$.

Figure 3 shows the behavior of eq 4, i.e., $\Theta = 0$, plotted as the tilt angle from the surface normal (γ) as a function of the dichroic ratio (D).

For comparison, the dichroic ratio for an isotropic distribution is given by

$$D = \frac{E_y^2}{E_x^2 + E_z^2} \tag{8}$$

By first determining the dichroic ratio experimentally, the average molecular tilt of the adsorbate from the *z*-axis can be estimated by solving eq 4 for γ. By comparing the experimental dichroic ratio with the isotropic value, it is possible to estimate the anisotropy of the adsorbate. A totally isotropic distribution of the molecules should yield a tilt angle of 54.7°. In the present work, a uniaxial distribution of the adsorbate was assumed.

Results and Discussion

Characterization by SEM, XRD, and Krypton Adsorption. The SEM images in Figure 4 are representative of the samples. The images show that the ZSM-5 film to a great extent consists of *b*-oriented crystals with tablet habit and that some parts of the element were not covered with film. Furthermore, most the crystals constitute a monolayer of intergrown crystals with a thickness of about 420 nm. A few crystals are deposited on top of this layer and a minor fraction of the crystals seems to be *a*-oriented twin crystals.

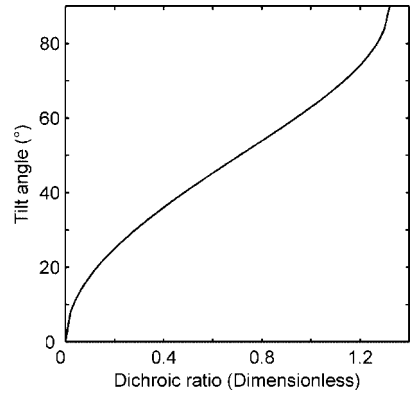

Figure 3. Tilt angle as a function of dichroic ratio as determined from eq 4.

The XRD pattern in Figure 5 shows that the film consists of almost only b-oriented crystals since merely reflections from *b*-planes are observed. This supports the SEM observations that showed that most of the crystals were *b*-oriented and indicated that only a small fraction of the crystals were *a*-oriented. The signal from a-oriented crystals (the (10 0 0) reflection)) may originate either from misaligned crystals or 90° rotational intergrowths and the low intensity of the (10 0 0) reflection as compared to the intensity of the (0 10 0) reflection, indicates that the amount of zeolite in 90° rotational intergrowths is very small as compared the amount of *b*-oriented zeolite. Consequently the effect of 90° rotational intergrowths on the adsorption measurements will be marginal. The XRD pattern is very similar to previously reported patterns for *b*-oriented MFI films.[57−59]

The preferred orientation of the crystals in the film was further studied by pole figure analysis of the (020) reflection, see Figure 6. The recorded intensity is represented by ten iso-intensity lines, the first line corresponds to 17% of the maximum intensity and for each additional line the intensity increases with 8%. Further, the guide circles are separated by 5° in Ψ. The data shows that the *b*-axis of most crystals deviate less than 15° from the surface normal, because almost all of the recorded intensity falls within $\Psi < 15°$. This shows that the vast majority of the crystals are *b*-oriented and ensures that the effect of misaligned crystals will be small. The data also indicates that the crystals are more tilted in the direction $\varphi = 90$ and 270°; however, this is most likely an artifact from the measurement and is reflecting the shape of the ATR element.

After calcination, the crystals were well-adhered to the support as they could not be removed mechanically without

(54) Ahn, D. J.; Franses, E. I. *J. Phys. Chem.* **1992**, *96* (24), 9952.
(55) Green, J. H. S. *Spectrochim. Acta* **1970**, *26A*, 1503.
(56) Neivandt, D. J.; Gee, M. L.; Hair, M. L.; Tripp, C. P. *J. Phys. Chem. B* **1998**, *102* (26), 5107.
(57) Jansen, J. C.; van Rosmalen, G. M. *J. Cryst. Growth* **1993**, *128*, 1150.
(58) Lai, Z. P.; Tsapatsis, M.; Nicolich, J. R. *Adv. Funct. Mater.* **2004**, *14* (7), 716.
(59) Wang, Z. B.; Yan, Y. S. *Chem. Mater.* **2001**, *13* (3), 1101.

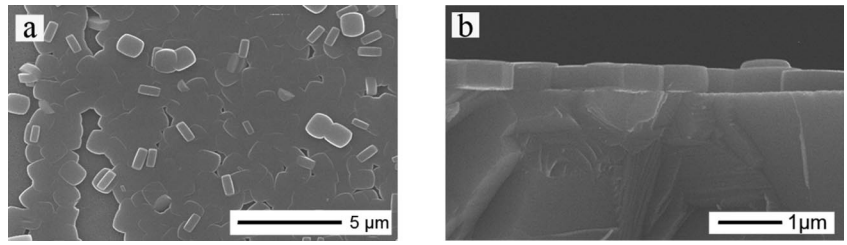

Figure 4. SEM images of ZSM-film on ZnS, (a) top- and (b) side-view.

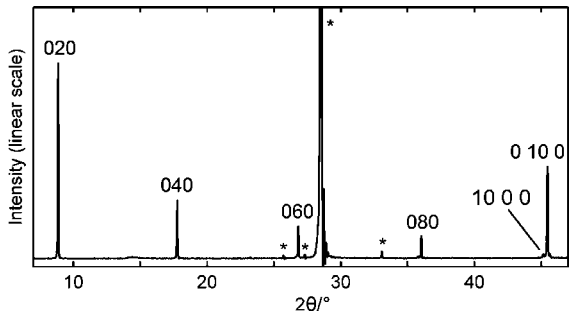

Figure 5. XRD pattern of the coated substrate. The indexed reflections emanates from the ZSM-5 film and the reflections labeled with * emanates from the ZnS element. The strong reflection at about 28.5° emanating from the ZnS element was ca. 25 times stronger than the (020) reflection of the ZSM-5 film.

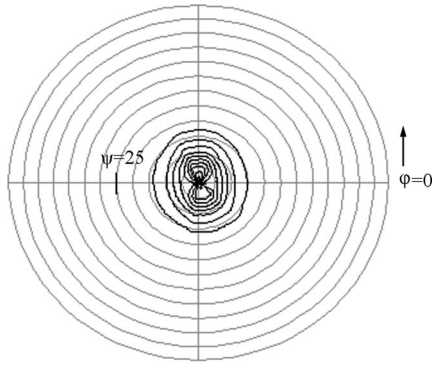

Figure 6. (020) pole figure of the ZSM-5 film on a ZnS ATR element.

damaging (scratching) the ATR element. The calcined film was rubbed both with a cotton stick and a piece of cloth pressed against the film with considerable force. Examination by SEM after the rubbing showed no traces of the film being removed. Consequently, the film was considered sufficiently stable for this application. However, our previous work indicates that the choice of material for the ATR element might affect the stability of the film.[46]

From the krypton adsorption measurements, a surface coverage of zeolite crystals on the ATR element could be determined to ca. 50%.

The ICP-SFMS measurements resulted in silicon and aluminum concentrations of 180 and 4.62 mg/g sample, respectively, yielding a Si/Al of 37.

FTIR/ATR Measurements. To investigate if uncoated parts of the element or *p*-xylene in gas phase influenced the measurements, adsorption of p-xylene on an uncoated element was first measured. A signal from the gas phase could only be detected at the highest partial pressure attainable with the experimental setup, i.e., 648 Pa. Figure 7 shows spectra recorded with an uncoated and a coated element recorded at 323 K and a *p*-xylene pressure of 648 Pa.

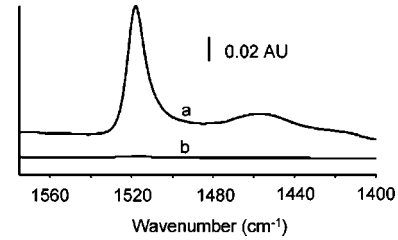

Figure 7. Part of spectra of *p*-xylene recorded at 323 K and 648 Pa. Spectrum (a) was recorded with a coated ATR element, whereas spectrum (b) was recorded with an uncoated element.

The peak height of the 1518 cm^{-1} band is about 84 times larger for the coated element. When considering that the only ca. 50% of the element is uncoated, the intensity of the peak recorded at 648 Pa emanating from the film should thus constitute more than 99% of the total intensity. Furthermore, the relative contribution from uncoated parts is highest at the highest pressure (worst case) and the contribution will be lower at all other pressures, it was thus concluded that *p*-xylene adsorbed on uncoated parts of the element and *p*-xylene in gas phase did not influence the measurements significantly.

The adsorption of p-xylene was first measured using nonpolarized light at 323 and 373 K. Figure 8 shows examples of spectra, recorded at 323 K without a polarizer and at *p*-xylene pressures of 0.8, 4.8, and 106 Pa.

The prominent absorption bands are indicated, and as expected, the intensity of the absorption bands increases with increasing *p*-xylene pressure in the feed. In the C−H stretching spectral region (2700−3100 cm^{-1}), several overlapping bands appear, from which two prominent bands are observed at 2926 and 2868 cm^{-1}. These bands have previously been assigned to C−H stretching vibration and to a C−H deformation overtone, respectively.[35] The adsorption of xylene on silanol groups has been reported previously.[60,61] Such adsorption is indicated by the data shown in Figure 8 (a) by the negative band at 3732 cm^{-1} accompanied with the appearance of a new band at 3580 cm^{-1}. In the region 1700−1400 cm^{-1}, a strong band appears at 1518 cm^{-1}assigned to stretching vibration of the aromatic ring.[35,55]

(60) Jentys, A.; Tanaka, H.; Lercher, J. A. *J. Phys. Chem. B* **2005**, *109* (6), 2254.
(61) Thibault-Starzyk, F.; Vimont, A.; Gilson, J.-P. *Catal. Today* **2001**, *70* (1−3), 227.

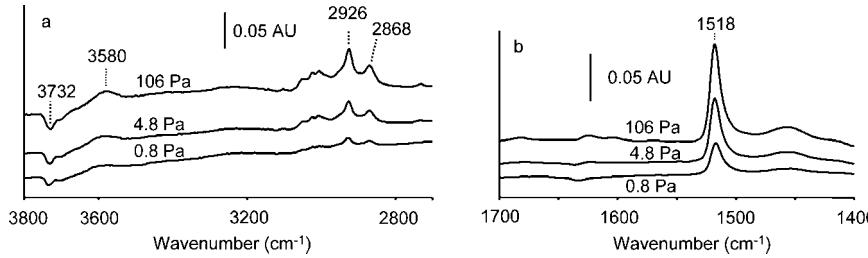

Figure 8. Spectra of *p*-xylene in the ZSM-5 film at different partial pressures recorded at 323 K using nonpolarized light.

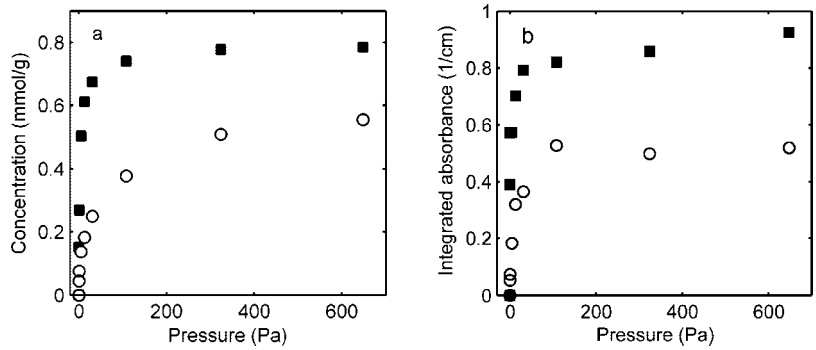

Figure 9. Adsorption isotherms of *p*-xylene in (a) ZSM-5 and (b) on silanol groups recorded at 323 K (□) and at 373 K (○).

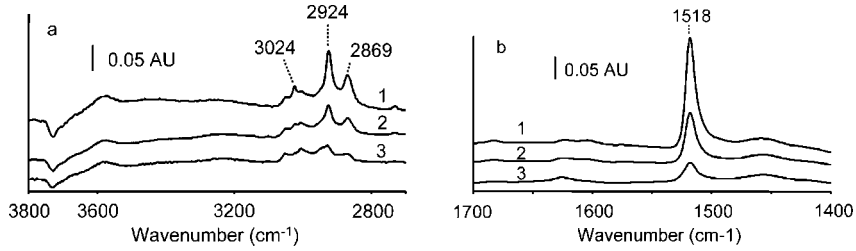

Figure 10. Parts of spectra of *p*-xylene recorded at $T = 323$ K and $P = 648$ Pa with p-polarized radiation (1), nonpolarized radiation (2), and with s-polarized radiation (3).

Isotherms for adsorption of p-xylene in the ZSM-5 pores extracted from the spectra by integrating the absorbance band at 1518 cm^{-1} by applying the same procedure as in our previous work[47] are presented in Figure 9a. The isotherms are very similar to the isotherms we reported for supported silicalite-1 films grown from seeds.[47] No step appears in the isotherm and only about half the saturation loading is reached, indicating that p-xylene only adsorbs in the intersections and does not adsorb in the sinusoidal channels. This is in accordance with previous results on films grown from seeds,[47] but in contrast to isotherms determined on powder and non supported films.[26,41,62] We speculate that the lack of a step in the isotherm may be either due to a size effect because our crystals are small or due to the bonding of the film to the support. The latter has previously been reported to induce strain in the film.[21−23]

Figure 9b shows the adsorption isotherm of p-xylene on silanol groups at 323 and 373 K extracted by integrating the negative absorbance band at 3732 cm^{-1}. Both plots resemble type I isotherms.

At each partial pressure, spectra were recorded with s- and p-polarized radiation as well, and examples of typical spectra are shown in Figure 10. Spectrum (1) is recorded with p-polarized radiation, spectrum (2) is recorded using nonpolarized radiation and spectrum (3) is recorded with s-polarized radiation, all spectra were recorded at 323 K and 648 Pa p-xylene in helium balance.

A strong polarization of several absorption bands is observed, and the most prominent of these bands are indicated in the figure. The indicated bands were assigned as follows:[35,55] 3024 cm^{-1}, stretching vibration of CH bonds in the aromatic ring; 2924 cm^{-1}, symmetric CH_3 stretching vibration; 2869 cm^{-1}, overtone of the asymmetric CH_3 deformation vibration; and 1518 cm^{-1}, aromatic ring stretching vibration. For all designated bands, much higher absorbance is obtained for the spectrum recorded with p-polarized radiation, indicating that there is a preferential orientation of the adsorbed molecules. Moreover, the designated bands are all assigned to vibrations having transition moments in the same direction,[35,55] i.e., in the same direction as the long axis of the molecule passing through the CH_3 groups. Consequently, the same trend is observed in both spectral regions shown in panels a and b in Figure 10. Figure 11a shows the dichroic ratio for the band at 1518 cm^{-1} as a function of concentration in the film at two temperatures.

At both temperatures, the dichroic ratio decreases with loading, indicating that the average tilt angle also decreases. Moreover, it can be seen that the slope of the curves are approximately the same in the concentration interval 0.25 to 0.5 mmol/g and that the limiting value at high concentrations seems to be similar at both temperatures. At lower

(62) Gelin, P.; Dutel, J. F.; Mentzen, B. F. *Microporous Mater.* **1995**, *4* (4), 283.

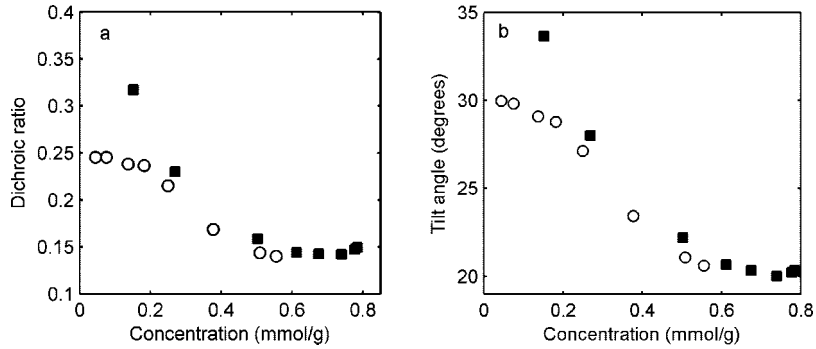

Figure 11. (a) Dichroic ratio for the band at 1518 cm^{-1} and (b) tilt angle as a function of concentration of *p*-xylene in the film recorded at 323 K (□) and at 373 K (○).

concentrations, the dichroic ratio at 373 K seems to reach a maximum value of about 0.25, whereas at 323 K the dichroic ratio reaches higher values. The tilt angles determined in this work from spectra and equations 27 are substantially lower than that for an isotropic distribution of the adsorbates of 54.7° showing that the molecules are mainly oriented with the long axis in the *b*-direction of the zeolite crystals. This is consistent with previous reports for low loadings of *p*-xylene in MFI, as was discussed in the introduction. The observed orientation is also similar to results obtained for several other para-substituted benzenes such as *p*-dichlorobenzene, *p*-chlorotoluene, and *p*-dibromobenzene. All these compounds show a similar adsorption behavior in MFI, where at low loadings, the molecules are adsorbed in the channel intersection with the long axis oriented mainly along the straight channels.[63−66]

The tilt angles estimated in this work at high pressures agrees well with the tilt angle of 18° as reported by Schüth[35] for *p*-xylene adsorbed in the intersections. In that work, the tilt angle was determined by IR microscopy on large crystals (380 × 70 μm) at ca. 310 K. In this context, it should also be mentioned that, as regarding determination of tilt angles with infrared spectroscopy, mobile adsorbates (i.e., the adsorbed molecules are not completely frozen) will result in tilt angles larger than 0°. Moreover, Mukti et al.[67] investigated the adsorption of *p*-xylene in the intersections of H/ZSM-5. The authors reported that at low loadings, the *p*-xylene molecules adsorbs preferentially on SiOHAl groups where the molecules are strongly constrained, whereas at higher loadings, the molecules take on a less constrained sorption geometry. The authors speculate that this might be due to intermolecular forces as neighboring intersections are occupied, this may perhaps explain the change in tilt angle with loading observed in the present work. As the external surface area of one crystal is relatively small (ca. 1%) as compared to the inner surface area, we believe that adsorption on the external surface would only have a very small effect on the measurements. As discussed previously, adsorption on silanol groups, internal and external, was indicated by the appearance of a negative band in the spectra in Figure 8. The adsorption on silanol groups might have influenced the results, but probably to a lesser degree.

The result from the present work, both the measurements conducted with polarized radiation and the isotherms support our previous findings, that at low temperatures, a type I isotherm appear with the *p*-xylene molecules mainly oriented in the *b*-direction of the zeolite crystals.[47]

Conclusions

b-Oriented ZSM-5 films were successfully grown on ZnS ATR-elements. Adsorption isotherms for *p*-xylene were measured at 323 and 373 K by FTIR/ATR spectroscopy. The isotherms resemble type 1 isotherms in concert with previous findings for supported films but in contrary to what have been reported for adsorption in MFI powder and unsupported films. Measurements with polarized radiation showed that the long axis of the *p*-xylene molecules where mainly oriented in the crystallographic *b*-direction. It was found that the tilt angle changed with loading, this might be due to different adsorption geometries in the pore system as reported previously. The tilt angle at higher loadings was in agreement with previously reported data determined by FTIR microscopy. Competitive adsorption on external silanol groups might also have affected the measurements, however, probably to a lesser degree.

The findings in this work show that care should be taken when extrapolating properties for zeolite powder as valid also for zeolite films, especially for systems where the adsorbate and the pores are of the same size.

This novel technique enabled, for the first time, following the tilt angle of *p*-xylene in ZSM-5 as a function of loading at two different temperatures. Further, the result also shows that this novel technique can be used for determining both adsorption isotherms as well as average molecular orientation in zeolites. The technique could also become a useful tool for studying anisotropic diffusion and multicomponent adsorption in zeolites, two research fields of very high importance.

Acknowledgment. The Swedish Research Council is gratefully acknowledged for financial support of this work and Peter Hedström at the Division of Materials Engineering is acknowledged for assisting with the pole figure measurements.

CM801399S

(63) Mentzen, B. F. *Mater. Res. Bull.* **1992**, *27*, 953.
(64) Mentzen, B. F.; Sacerdote-Peronnet, M. *Mater. Res. Bull.* **1993**, *28*, 1161.
(65) van Koningsveld, H.; Jansen, J. C.; van Bekkum, H. *Acta Crystallogr., Sect. B* **1996**, *52*, 140.
(66) Fyfe, C. A.; Brouwer, D. H. *J. Am. Chem. Soc.* **2006**, *128*, 11860.
(67) Mukti, R. R.; Jentys, A.; Lercher, J. A. *J. Phys. Chem. C* **2007**, *111*, 3973.